that strings also produce double images). We see that the ambiguity in relative velocities results in a discontinuity in the Doppler shift of a source behind the string. Thus, there will be discontinuities in the microwave background temperature at positions on the sky where strings with relativistic transverse velocities are located. It is this discontinuity in temperature along curves in the sky which is peculiar to strings. This effect has been noted independently by Gott[11].

In the rest frame of the string all particles passing the string are deflected by an angle of $8\pi G\mu$ with respect to particles passing on the other side of the string. Unlike usual gravitational lenses, this deflection is independent of impact parameter as long as the impact parameter is much smaller than the radius of curvature of the string. Thus the magnitude of the discontinuity in temperature across the string is $\delta T/T = 8\pi G\mu\beta$ where β is the transverse velocity of the string which will typically be close to unity. This jump in temperature will persist an angular distance away from the string corresponding to the apparent angular size of the radius of curvature of the string. The magnitude of the temperature jump is independent of the redshift at which the light rays reaching us passed by the string.

The number density of discontinuities on the sky depends on the number of loops appearing on the horizon per expansion time which is determined by the efficiency of intercommutation. However, it is difficult to see how this process could cause the number of horizon size lengths of string per horizon volume to decrease below unity. We thus consider one horizon size length of string per horizon size to be the minimal model for the production of anisotropy.

We wish to calculate the general properties of the microwave sky anisotropy in this minimal model. Let us assume that the microwave photons were last scattered at redshift z_{ls}. In a perfectly homogeneous universe, the matter becomes mostly neutral and optically thin at $z \sim 1{,}000$. However, in a universe with strings, there will be large-amplitude inhomogeneity on small scales and the heat input from objects forming at or before z_{rec} may reionize the plasma[8]. If the plasma were kept fully ionized then $z_{ls} > 10$, so we must have $1{,}000 > z_{ls} > 10$. The angle subtended by a horizon-sized volume of space at z_{ls} is $\theta_{ls} \sim z_{ls}^{-1/2} \ll 1$. What do we expect to see on a round patch of sky of diameter $\theta > z_{ls}^{-1/2}$? It is clear that the one horizon size length of string per horizon volume at redshift z will project to one length of string of angular size θ if $z < z_{ls}$. These strings will be moving relativistically as they were unable to straighten themselves out on these length scales before this epoch but will be smooth on scales smaller than this. Thus these strings will produce line-like discontinuities in temperature with $\delta T/T \sim 8\pi G\mu$ which persist for an angle $\sim\theta$ away from the line.

Also projected on the sky will be relativistically oscillating loops which have already entered the horizon. However, in our minimal model one can show that the angular distance between such sub-horizon loops is much greater than their angular size. Thus, in a beam switching experiment with beam width and beam throw $\sim\theta$ it is unlikely that the beam throw would straddle a sub-horizon loop, but if $\theta > \theta_{ls}$ it would probably straddle a horizon size loop. Such an experiment would average over any anisotropy due to loops with projected size smaller than θ and would only be sensitive to strings with projected angle of curvature $\sim\theta$. For the minimal model we conclude that a beam switching experiment on angular scales $\theta > z_{ls}^{-1/2}$ rad would see temperature deviations with magnitude $\sim 8\pi G\mu$, due mostly to horizon-sized lengths of string. As such experiments have already been done which do not detect anisotropy of magnitude 10^{-4} (ref. 10) on angular scales $>10°$, we conclude that $G\mu < 10^{-5}$ if any strings exist. For purposes of galaxy formation, $G\mu \approx 10^{-6}$ has been suggested[5]. If more strings exist than in our minimal model then an even greater anisotropy of $\sim\sqrt{N_s}\,8\pi G\mu$ would be produced, where N_s is the mean number of overlapping loops of a given size. If anisotropy is ever detected, one could determine whether it was due to strings by looking for line-like temperature discontinuities on the sky. From the magnitude of the discontinuities one can read off the microphysical parameter μ. If strings were found in this way it would test the theory of general relativity for stress–energy tensors unlike those of ordinary matter, as well as confirm some ideas about non-perturbative quantum field theories.

Received 23 April; accepted 24 May 1984.

1. Kibble, T. W. B. *J. Phys.* A9, 1387–1398 (1976).
2. Vilenkin, A. *Phys. Rev.* D23, 852–857 (1981).
3. Everett, A. E. *Phys. Rev.* D24, 858–868 (1981).
4. Vilenkin, A. *Phys. Rev.* D24, 2082–2089 (1981).
5. Vilenkin, A. & Shafi, Q. *Phys. Rev. Lett.* 51, 1716–1719 (1983).
6. Turok, N. Preprint, *Grand Unified Strings and Galaxy Formation* (Univ. California, Santa Barbara, 1984).
7. Turok, N. Preprint, *Stretching Cosmic Strings* (Univ. California, Santa Barbara, 1984).
8. Hogan, C. Preprint, *Massive Black Holes Generated by Cosmic Strings* (Caltech, 1984).
9. Birkinshaw, M. & Gull, S. F. *Nature* 302, 315–317 (1983).
10. Fixsen, D. J., Cheng, E. S. & Wilkinson, D. T. *Phys. Rev. Lett.* 50, 620–622 (1983).
11. Gott, J. R. Preprint, *Gravitational Leasing Effects of Vacuum Strings: Exact Solutions* (Princeton Univ., 1984).

'Melting ice' I at 77 K and 10 kbar: a new method of making amorphous solids

O. Mishima, L. D. Calvert & E. Whalley

Division of Chemistry, National Research Council, Ottawa, Canada K1A 0R9

Amorphous solids are made mainly by cooling the liquid below the glass transition without crystallizing it, a method used since before recorded history[1], and by depositing the vapour onto a cold plate[2], as well as by several other methods[3,4]. We report here a new way—by 'melting' a solid by pressure below the glass transition of the liquid—and apply it to making a new kind of amorphous ice. Thus, ice I has been transformed to an amorphous phase, as determined by X-ray diffraction, by pressurizing it at 77 K to its extrapolated melting point of 10 kbar. At the melting point, the fluid is well below its glass transition. On heating at a rate of ~2.6 K min^{-1} at zero pressure it transforms at ~117 K to a second amorphous phase with a heat evolution of 42 ± ~8 J g^{-1}, and at ~152 K further transforms to ice I with a heat evolution of 92 ± ~15 J g^{-1}. In one sample, ice Ic was formed and in another, existing crystals of ice Ih grew from the amorphous phase. Heating below the 117 K transition causes irreversible changes in the diffraction pattern, and a continuous range of amorphous phases can be made. Similar transformations will probably occur in all solids whose melting point decreases with increasing pressure if they can be cooled sufficiently for a transformation to a crystalline solid to be too slow.

Several solids, such as ice I, melt with a decrease of volume, and so the melting temperature falls as the pressure increases. The melting line usually ends at a triple point, where another solid phase becomes stable, but, as the solid–liquid transition is first-order, it can, in principle, be extrapolated to low temperature and even to zero temperature. It follows that if such a solid is compressed at a temperature that is low enough to prevent transformation to another crystalline phase, it must either 'melt', perhaps to an amorphous solid if it is below the glass transition of the liquid, or become a crystal that is greatly superheated into the liquid region. Either case would be new and could be of great interest. The melting curve of ice Ih extrapolates to ~10 kbar at 77 K (Fig. 1); we have therefore squeezed ice Ih at 77 K and have examined the product that is recovered at zero pressure by determining its density, by thermal analysis, and by X-ray diffraction.

Figure 2 plots the compression for four different runs against the nominal pressure, assuming no friction. In each run, a transition started at an estimated real pressure of 10 ± ~1 kbar and appeared complete by ~15 kbar. About two-thirds of the volume change occurred in a pressure range of ~0.7 kbar. The transition goes surprisingly easily for such a low temperature. For comparison, a similar sample of ice IX at the same temperature did not transform below 25 kbar, although it is always metastable relative to ice II and also becomes metastable relative to ice VI

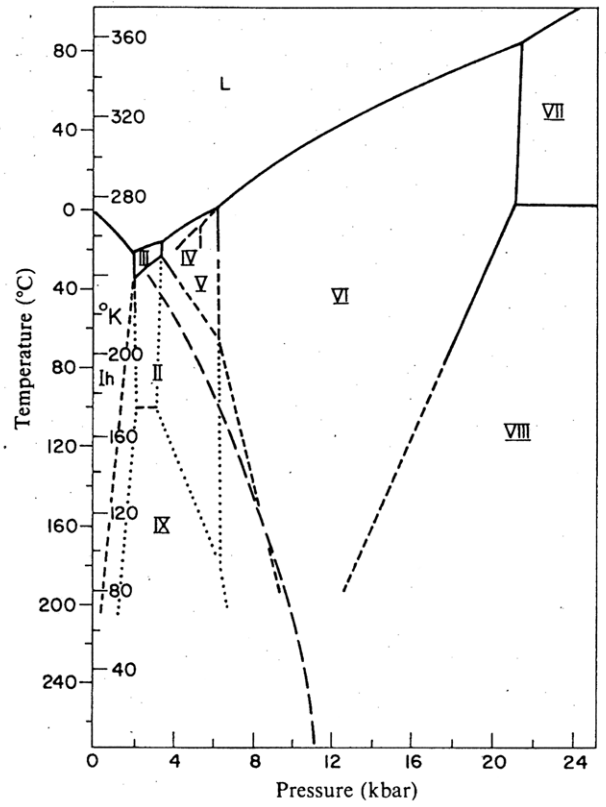

Fig. 1 The phase diagram of ice in the pressure–temperature plane. The melting line of ice I is extrapolated as a dashed line.

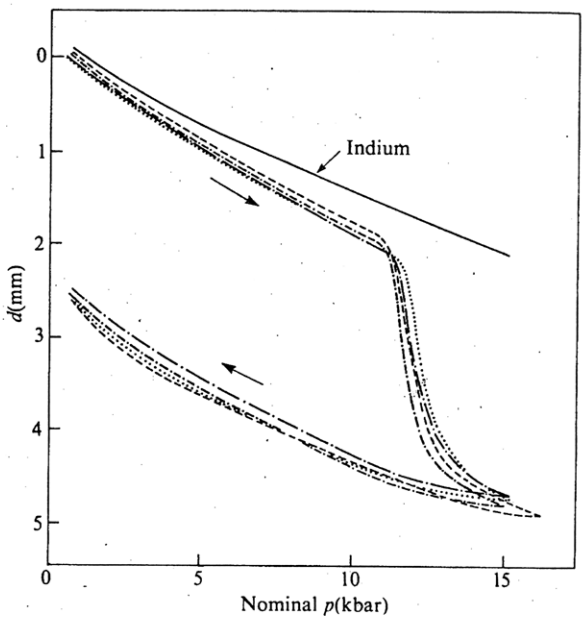

Fig. 2 Compression of ice I as a function of the nominal pressure on the sample for four independent runs at 77 K and on a volume of indium equal to the volume of the indium cup and the ice. About 1.2 cm^3 of water in an indium cup was compressed in a steel cylinder by a hydraulic press and the displacement d of the piston was measured to 2.5 μm by a dial gauge as a function of the nominal pressure p. The pressure of the sample is ~0.9 of the nominal pressure. The measured compression was used with the compression of an equal volume of indium[17] to determine the compression of the ice.

at ~9.4 kbar and to ice VIII at ~12.3 kbar. The ease with which ice I transforms at ~10 kbar is, therefore, quite unprecedented. The specific volumes of liquid water, ice and the new phase as a function of pressure are represented in Fig. 3, which may be read in conjunction with Fig. 1. The specific volume at 77 K of ice I and of the new phase, both at 10 kbar, are consistent with the extrapolated specific volumes of ice I on the liquid-I line (labelled *a*), of the liquid on the liquid-I line (labelled *c*) and of the liquid along the 9.8-kbar isobar (labelled *d*) where the dotted lines are extrapolations. The relation of the new phase to the amorphous ice made by quenching the liquid can be understood by the extrapolation of the liquid along the 1 bar isobar (labelled *b*).

Figure 4 shows a first-order plot of the heating curve of the recovered phase. There are exothermic events starting at ~117 and ~152 K, at a heating rate of ~2.6 K min^{-1}, with a heat evolution, from two independent experiments, of 42 ± ~8 and 92 ± ~15 J g^{-1}, respectively.

Two specimens were analysed by X-ray powder diffraction at ~95 K[5], and microphotometer traces of representative patterns of the second are reproduced in Fig. 5. Both specimens as recovered had a halo pattern typical of an amorphous material, having its main peak at 3.0 Å and with rings and spots ascribable to a small amount of untransformed ice Ih. After heating the first specimen, which was a powder, to ~130 and ~170 K and cooling to 95 K, the halo pattern was replaced by a ring pattern typical of ice Ic, and the ice Ih pattern remained. After heating to ~200 K, only the ice Ih pattern remained, and the original Ih crystals had clearly grown.

The second specimen was a euhedral fragment ~0.4 mm on edge with a small amount of powder. The principal halo was a broad peak at 3.0 Å; it narrowed and its position, as measured at ~95 K, shifted almost linearly with heating temperature, from 3.0 to 3.65 Å after heating successively to ~105, ~112 and ~135 K for ~10 min and further shifted to 3.67 Å after heating to 155 K. After heating to ~175 K for ~20 min, the halo pattern disappeared and the Ih spots grew considerably, but no Ic pattern was produced. This appears to be the first report of the direct transformation of amorphous ice to ice Ih instead of Ic. The conditions no doubt gave preference to growth of Ih crystals against nucleation of Ic.

The first halo pattern is undoubtedly of a new dense amorphous solid having its principal peak at ~3.0 Å; this is much smaller than that of the first ice-Ih triplet centred at 3.65 Å or the principal peak of amorphous ice made by condensing the vapour[6–9] or rapidly cooling liquid water[10]. The bands are rather broad, showing that the interatomic correlations are relatively weak. When this phase is heated successively to ~105, ~112 and ~135 K, the halo moves to longer spacings, the bands become narrower and a discontinuous change occurs at ~117 K, as shown by the heating curves. The discontinuous change is probably caused by 'runaway' heating. The phase so produced resembles the amorphous ice made by condensing the vapour or quenching the liquid.

It seems clear that a new amorphous phase of ice of density about 1.31 g cm^{-3} is produced by the transformation of ice Ih at 77 K and 10 kbar, near its extrapolated melting point. Its volume appears to increase reversibly on removing the pressure and its density decreases to 1.17 g cm^{-3}, which is about 26% denser than the films made by condensing the vapour in the range 82–110 K[11]. On heating, it transforms irreversibly in stages towards a phase that in some ways resembles amorphous ice made by condensing the vapour or quenching the liquid but is clearly different from it, and a discontinous exothermic change occurs at ~117 K at our heating rate of ~2.6 K min^{-1}. A wide range of amorphous phases could probably be made by carefully controlled heating.

Amorphous solids can now be made in several ways, and at least four of them have been used to make amorphous phases of ice: condensing the vapour at low temperature, quenching the liquid, transforming the crystal at high pressure below the glass transition of the liquid, and warming the amorphous phase so produced. Each of them can be used to make phases with a range of properties depending on the conditions, and further

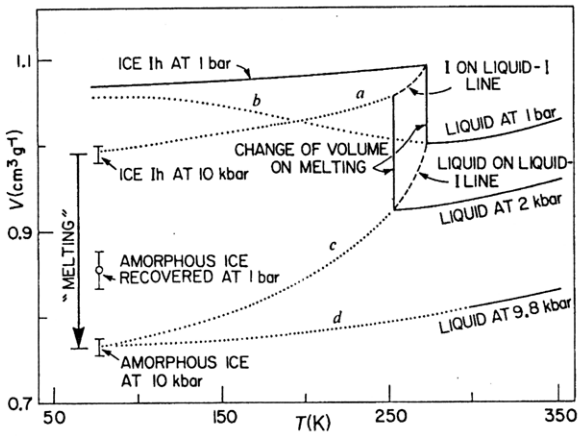

Fig. 3 Graph of the specific volume of ice I at 1 bar, ice I on the liquid-I line (labelled *a*), the liquid at 1 bar (labelled *b*), the liquid along the melting curve from 0 to 2 kbar (labelled *c*), the liquid at 9.8 kbar (labelled *d*), and reasonable extrapolations to 77 K. Measured values are represented by full and dashed lines and extrapolated values by dotted lines. The densities of ice Ih and of the new phase at 77 K and 10 kbar as determined from the compression experiments, and of the new phase (two samples) at 77 K and zero pressure as measured by weighing in liquid and gaseous nitrogen, are also plotted.

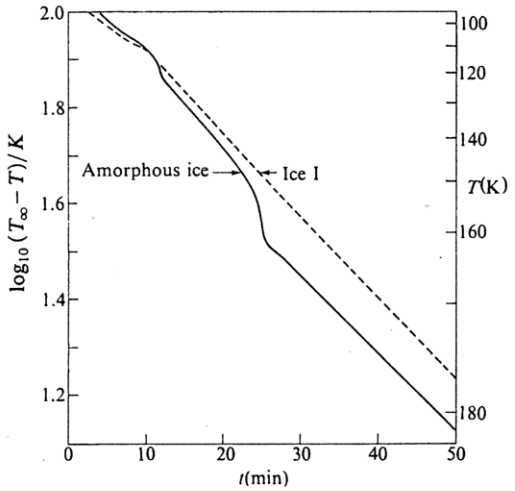

Fig. 4 The first-order plot of a heating curve of the recovered phase. The sample was held in a small silvered glass vacuum flask[5] immersed in a bath of ethanol and carbon dioxide. The heating rate was ~2.6 K min^{-1}.

studies of them should tell much about how water molecules interact with one another. A possible nomenclature to distinguish the different methods of preparation is amorph-v, amorph-l and amorph-c for the phases made from the vapour, liquid and crystal, respectively, and amorph-c-h for the phases made by heating the phase obtained by transforming the crystal at low temperature.

The transformation crystal-to-amorph-c is obtained surprisingly easily for such a low temperature. This suggests that the crystal becomes unstable and transforms, presumably at its surface, to a phase resembling the supercooled liquid. It is not reversible on the ordinary laboratory time scale and so is not a true melting, and may be viewed as a new kind of transition—an easy transformation of a crystalline solid to a dense amorphous solid.

Similar transformations will probably occur in all solids that have negative volumes of melting when a transformation to a crystalline solid is too slow. Obvious examples are the structure II clathrate hydrates, specifically tetrahydrofuran clathrate hydrate[12], ammonium fluoride I[13], ammonium fluoride monohydrate, indium antimonide[14] and germanium[15], which may transform to an amorphous phase at ~10, ~20, ~20, ~50 and ~170 kbar, respectively, at 77 K. Other obvious candidates for amorphization in this way are graphite, diamond, silicon, germanium, cubic and hexagonal boron nitride and phosphide, and graphite-like boron nitride. A transformation to an amorphous phase, rather than to a supposed metallic crystalline form, may limit the maximum force that can be applied to diamond and other tetrahedral compounds at low temperatures and so limit the pressures attainable in diamond anvil apparatuses. The transformation crystal-to-amorph-c in ice and clathrate hydrates may occur in planets formed by the agglomeration of cold particles of ice I or clathrate hydrate.

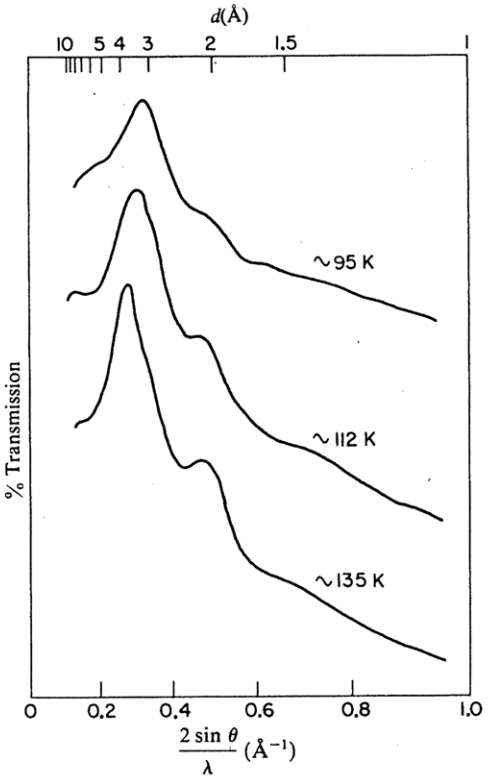

Fig. 5 Representative microphotometer tracings of diffraction patterns of a homogeneous sample of the new phase taken in a flat-plate X-ray camera. The temperature was controlled to ±~5 K by flowing nitrogen gas and was measured by a thermocouple placed near the specimen. Photographs were taken at ~95 K using zironium-filtered molybdenum radiation[5].

An obvious way to transform an asymmetrical to a symmetrical hydrogen bond is to squeeze ice I[16]. To compress the O–O distance of 2.75 Å to the ~2.4 Å needed for centrosymmetrical bonds would require only some tens of kilobars. Unfortunately, ice transforms to the amorphous phase at much lower pressures.

National Research Council contribution no. 23539.

Received 20 February; accepted 9 May 1984.

1. Morey, A. W. *The Properties of Glass* 2nd edn, Ch. 1 (Reinhold, New York, 1954).
2. Tammann, G. & Starinkewitsch, J. *Z. phys. Chem.* **85**, 573–578 (1913).
3. Secrist, D. R. & McKenzie, J. D. in *Modern Aspects of the Vitreous State* Vol. 3, 149–165 (Butterworths, London, 1964).
4. De Carli, P. S. & Jamieson, J. C. *J. chem. Phys.* **31**, 1675–1676 (1959).
5. Bertie, J. E., Calvert, L. D. & Whalley, E. *J. chem. Phys.* **38**, 840–846 (1963).
6. Burton, E. F. & Oliver, W. F. *Proc. R. Soc.* **A153**, 166–172 (1938).
7. Dowell, L. G. & Rinfret, A. P. *Nature* **188**, 1144–1148 (1960).
8. Bondot, P. *C.r. hebd. Séanc. Acad. Sci., Paris* **265**, 316–318 (1967).
9. Narten, A. H., Venkatesh, C. G. & Rice, S. A. *J. chem. Phys.* **64**, 1106–1121 (1976).
10. Mayer, E. & Brügeller, P. *Nature* **298**, 715–718 (1982).
11. Ghormley, J. A. & Hochandel, C. J. *Science* **171**, 62–64 (1971).
12. Gough, R. & Davidson, D. W. *Can. J. Chem.* **49**, 2691–2699 (1971).
13. Kuriakose, A. K. & Whalley, E. *J. Chem. Phys.* **48**, 2025–2031 (1968).
14. Merrill, Leo. *J. phys. Chem. Ref. Data* **6**, 1205–1252 (1977).
15. Cannon, J. F. *J. phys. Chem. Ref. Data* **3**, 798–824 (1974).
16. Stillinger, F. H. & Schweitzer, K. S. *J. phys. Chem.* **87**, 4281–4288 (1983).
17. Bridgman, P. W. *Proc. Am. Acad. Arts Sci.* **76**, 9–24 (1945).